Electronic Supplementary Material (ESI) for Environmental Science: Nano.

Supporting information

Intracellular Trafficking of Silver Nanoparticles and Silver Ions Determined their Specific Mitotoxicity to Zebrafish Cell Line

Neng Yan[a], Ben Zhong Tang[b], Wen-Xiong Wang[a,c*]

[a] *School of Energy and Environment, State Key Laboratory of Marine Pollution, City University of Hong Kong, Kowloon, Hong Kong, PR China*

[b]*Department of Chemistry, Hong Kong Branch of Chinese National Engineering Research Center for Tissue Restoration and Reconstruction, HKUST, Clear Water Bay, Kowloon, Hong Kong, China*

[c]*Research Centre for the Oceans and Human Health, City University of Hong Kong Shenzhen Research Institute, Shenzhen 518057, China*

*Corresponding author, Email: wx.wang@cityu.edu.hk

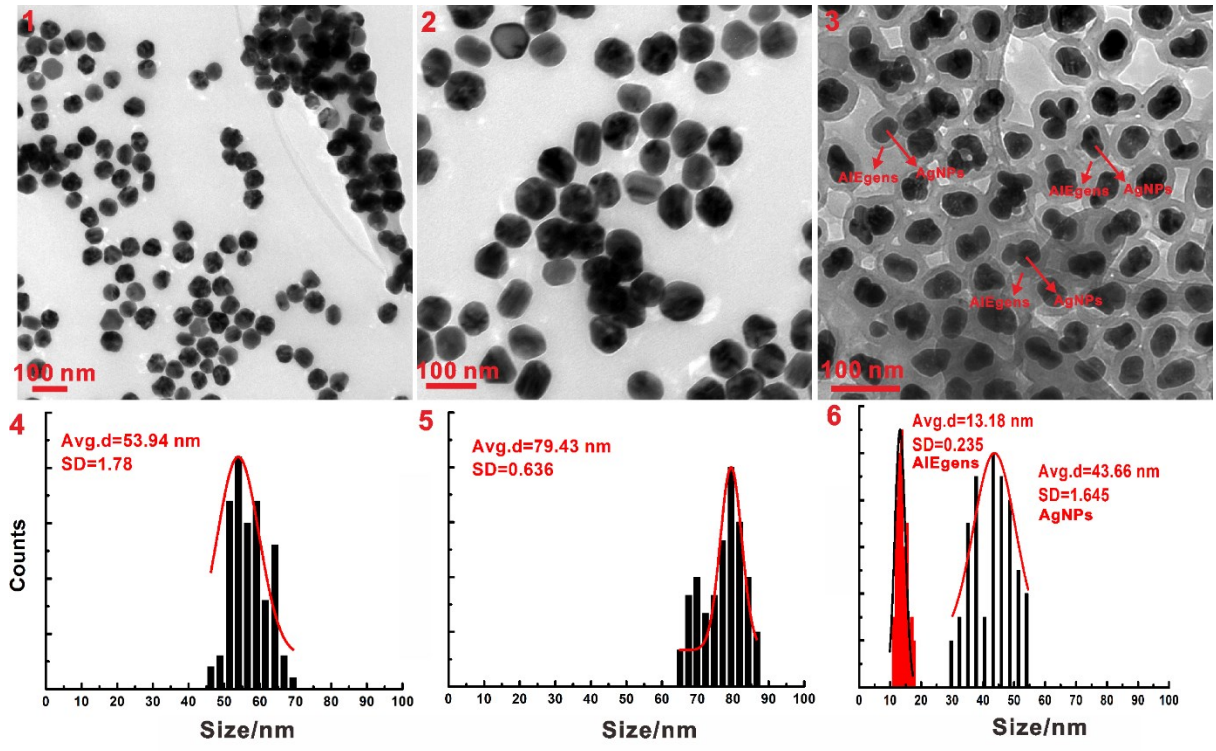

Figure S1. Characterization of synthesized AgNPs. (1) TEM images of Cit-AgNPs-1. (2) TEM images of Cit-AgNPs-2. (3) TEM images of AIE-AgNPs with distinct core part (AgNPs) and surface coating (AIEgen) as denoted by red arrows. (4) Size distribution of Cit-AgNPs-1, with the size is 53.94 nm, and the standard error (SD) of 1.78 nm (n=100). (5) Size distribution of Cit-AgNPs-2, with the size is 79.43 nm, and the SD of 0.636 nm (n=60). (6) Size distribution of surface coating AIEgens (Size, 13.18; SD, 0.235) and core part (AgNPs) (Size, 43.66 nm; SD,1.645 nm) (n=60).

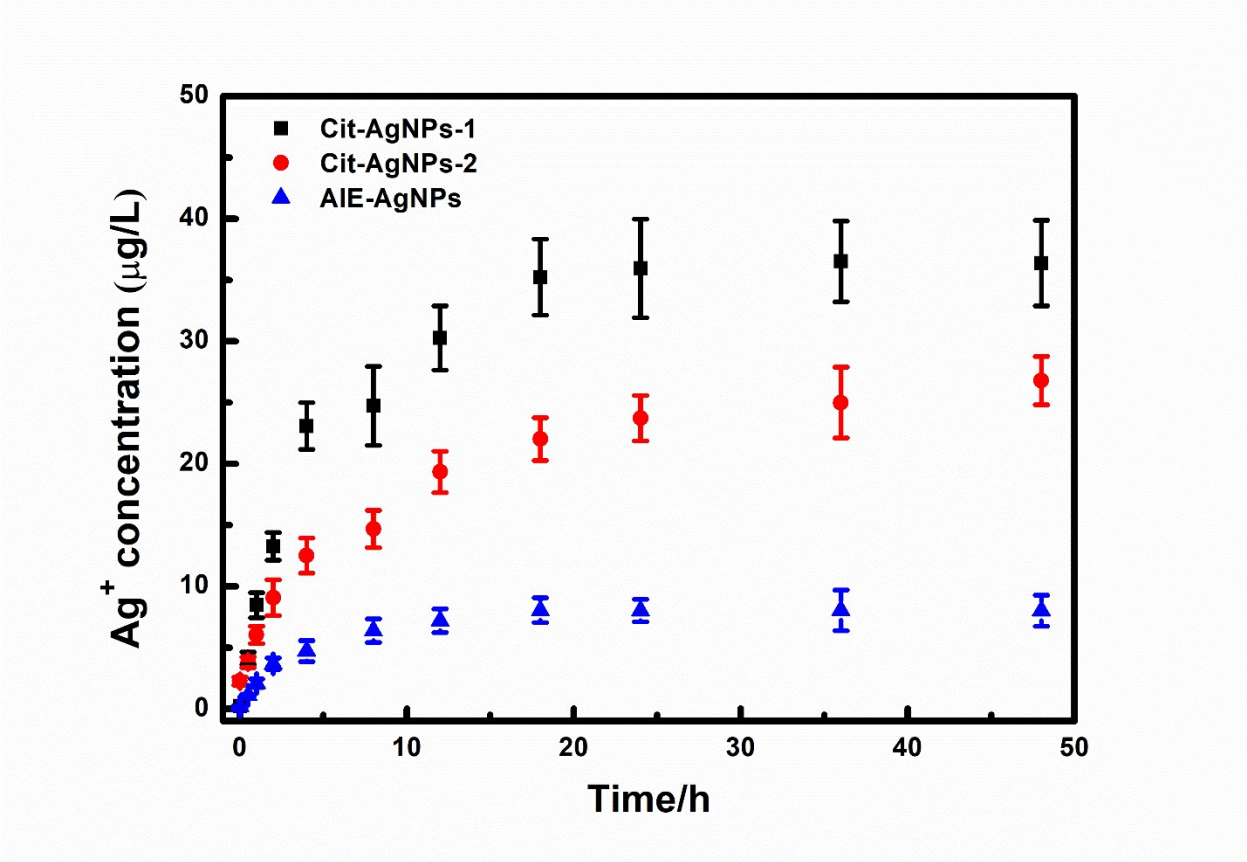

Figure S2. Dissolution kinetics of 500 μg/L of Cit-AgNPs and AIE-AgNPs in SM7 medium (pH=7.0).

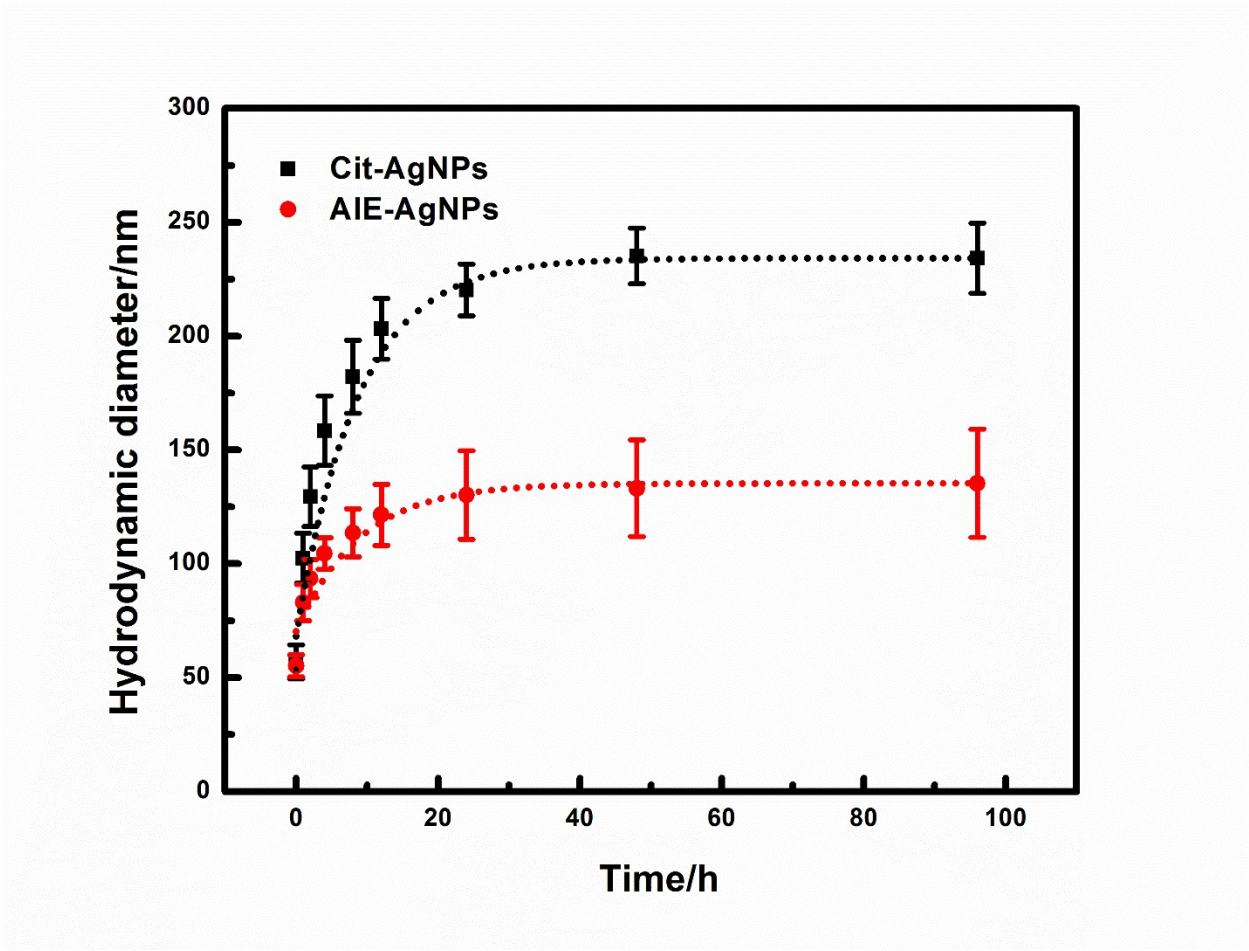

Figure S3. Aggregation kinetics of AIE-AgNPs and Cit-AgNPs-1 (500 μg/L) in the SM7 medium.

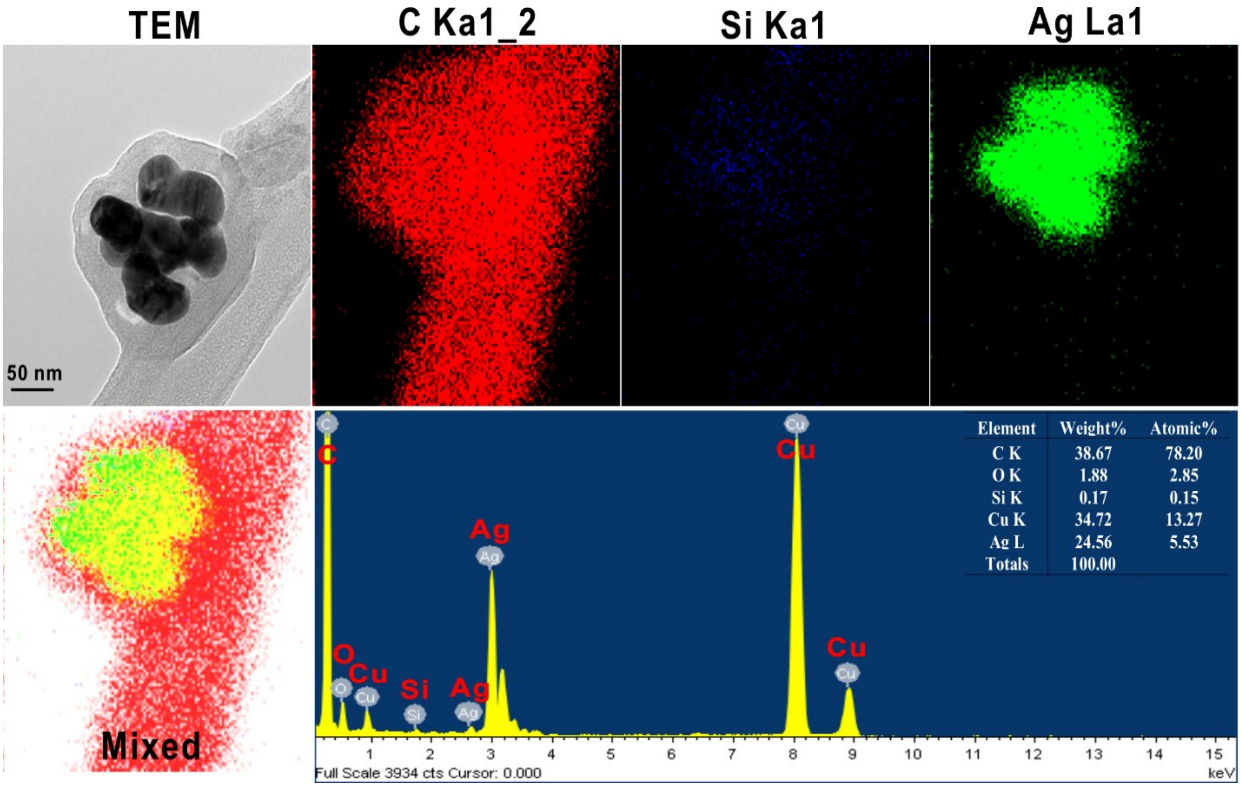

Figure S4. TEM images of aggregated AIE-AgNPs accumulated in SM7 medium and the EDX mapping of selected elements (Ag, C and Si).

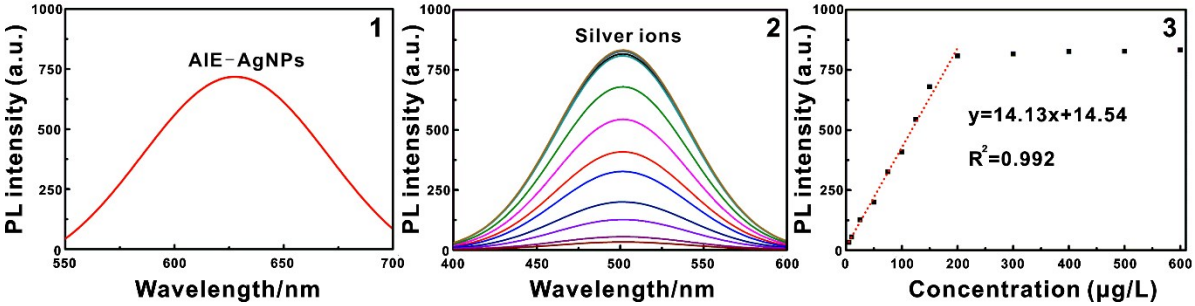

Figure S5. Fluorescence properties of AIE materials. (1) Emission of the AIE-AgNPs in SM7 medium, λ_{ex}=450 nm. (2) Emission of the TEZ-TPE-1 with different concentration of Ag^{+}, λ_{ex}=365 nm. (3) Fluorescence intensity (I 501 nm) vs the concentration of Ag^{+}.

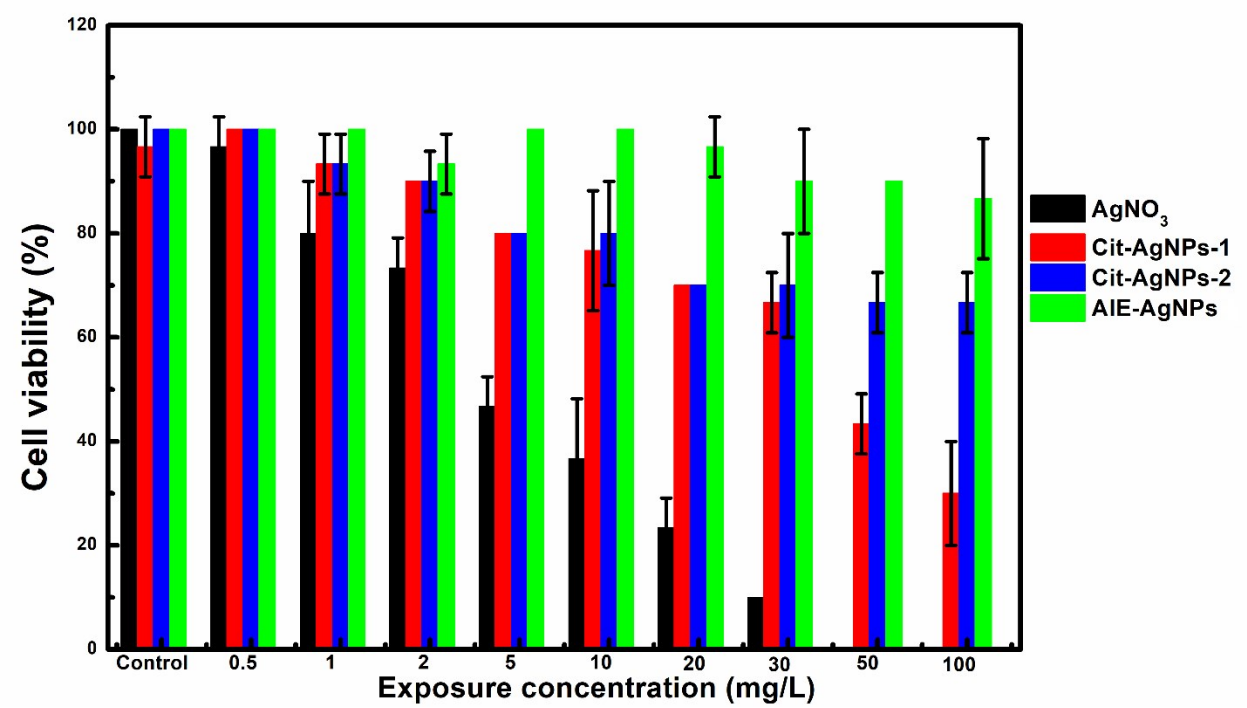

Figure S6. Percentage viability of cells upon treatment with $AgNO_3$ and AgNPs by PrestoBlue test. The AgNPs exposure concentrations used in the study were 0, 0.5, 1, 2, 5, 10, 20, 30, 50 and 100 mg/L. Data are expressed as mean ± SE (n=5).

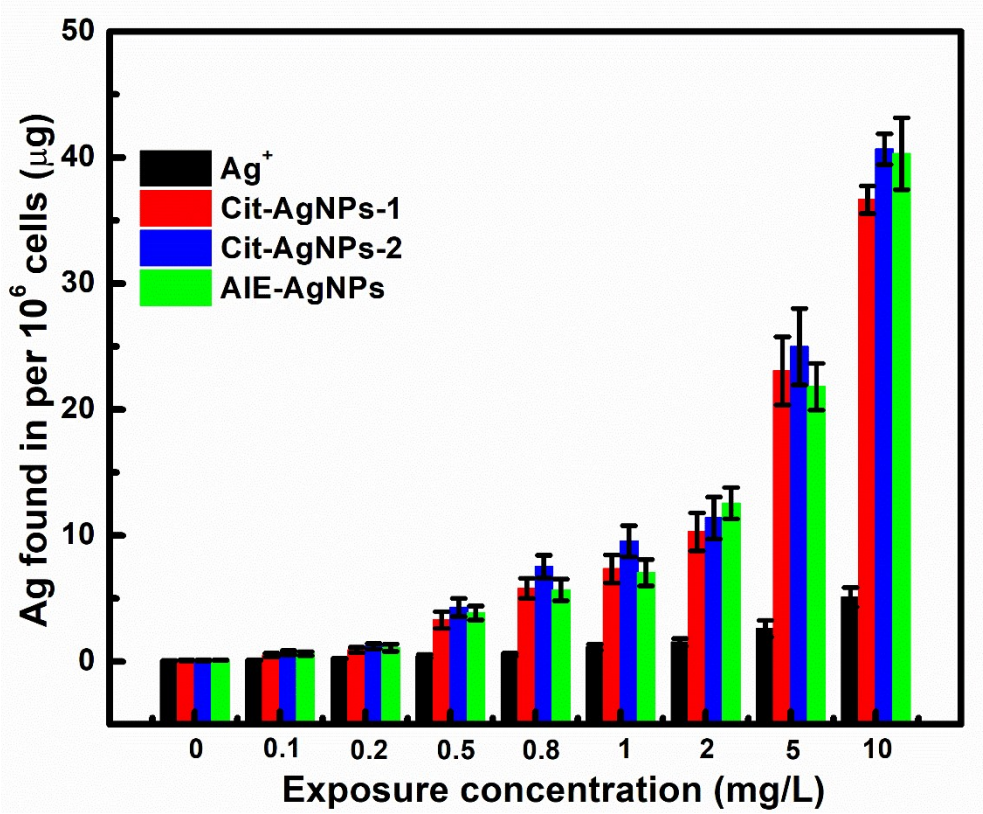

Figure S7. Bioaccumulation of AgNPs (AIE-AgNPs and Cit-AgNPs) and $AgNO_3$ in ZF4 cell lines exposed at different concentration after 24h exposure. Significant difference is found between Ag^+ and AgNPs (both Cit-AgNPs and AIE-AgNPs) exposure groups (*$P < 0.05$) while no significance difference was found between Cit-AgNPs and AIE-AgNPs exposure groups ($P > 0.05$).

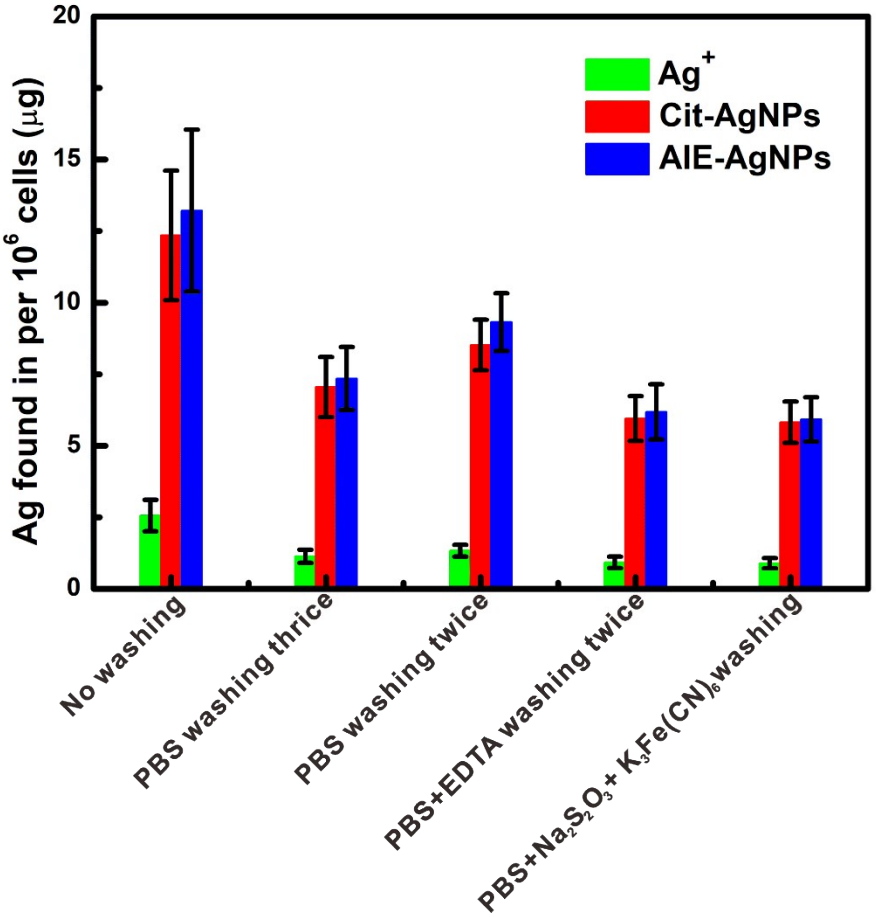

Figure S8. Bioaccumulated AgNPs in ZF4 cell lines after exposed to AgNPs (AIE-AgNPs and Cit-AgNPs-1) and $AgNO_3$ for 24 h followed with different washing methods reported in previous studies.[1-4] While significant difference was found between washing and non-washing groups for both the AgNPs (***$p<0.0005$) and $AgNO_3$ (***$p<0.0005$) exposure, no significant difference was found between different washing methods between the method used in present study and convenient methods.

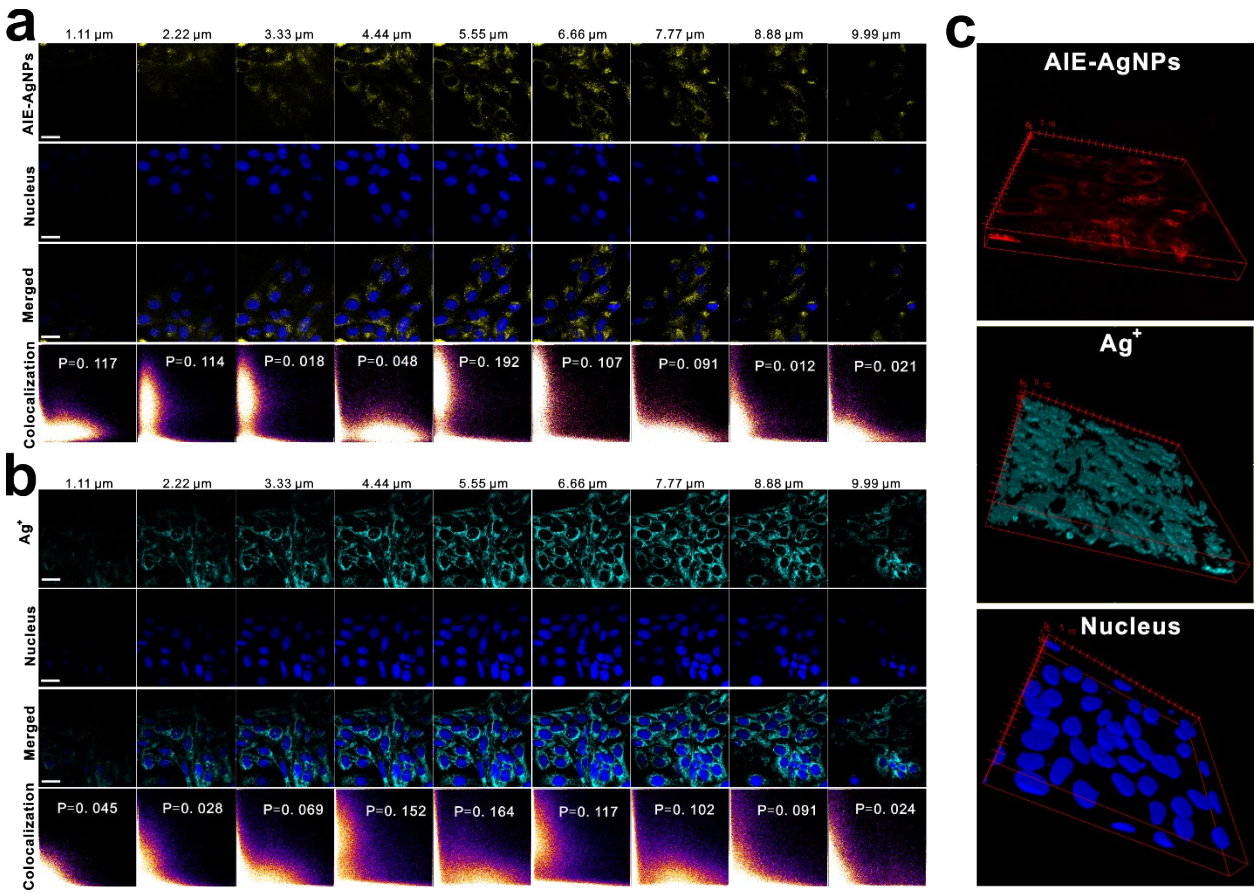

Figure S9. 3D confocal images of cells with different channels. AIE-AgNPs and nucleus (a), the dissolved Ag^+ with nucleus (b) and 3D reconstruction of cells with AIE-AgNPs-1, Ag^+ and nucleus channels. The scale bar is 20 μm.

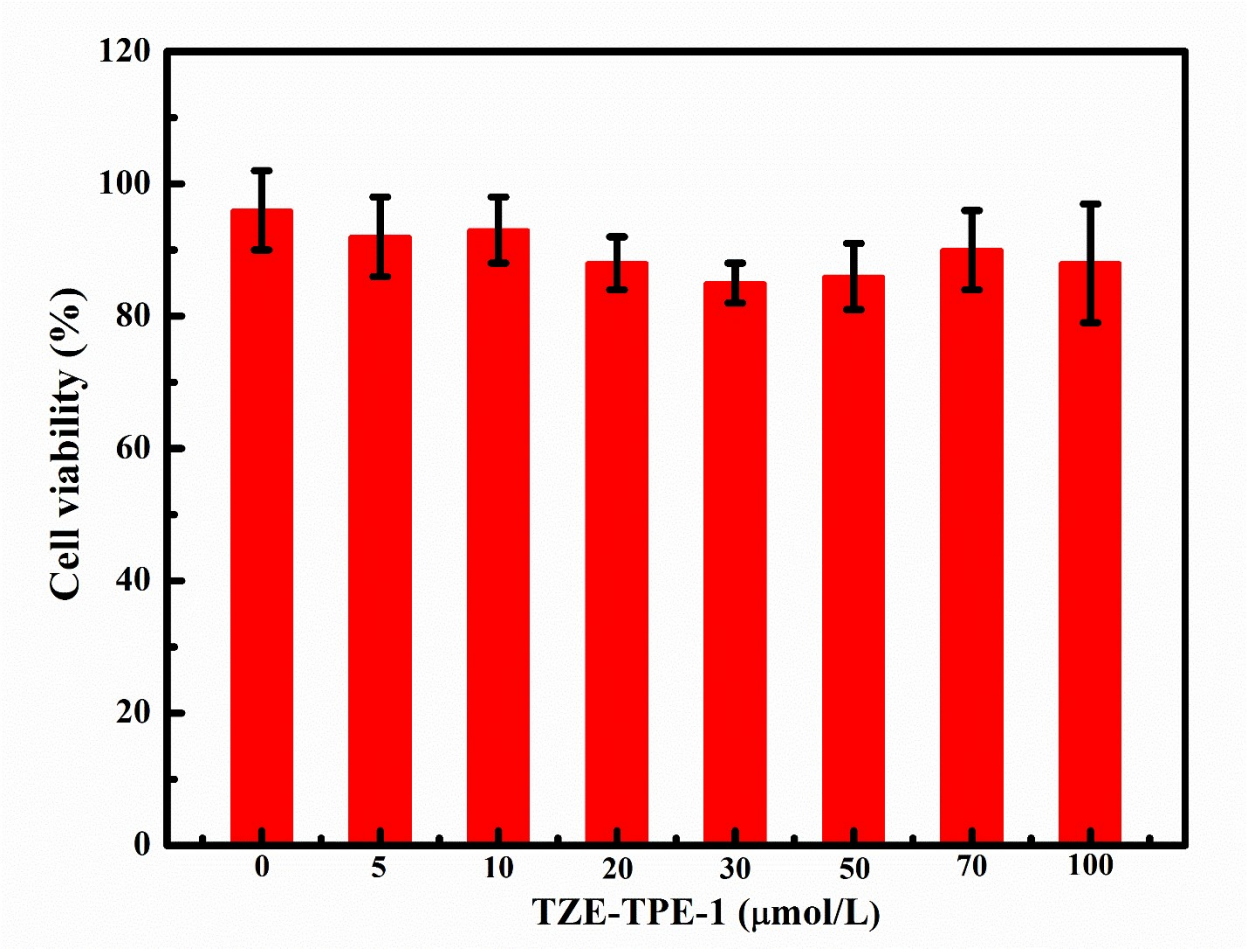

Figure S10. Effect of different doses of TEZ-TPE-1 on the viability of ZF4 cell lines assessed by the MTT assay.

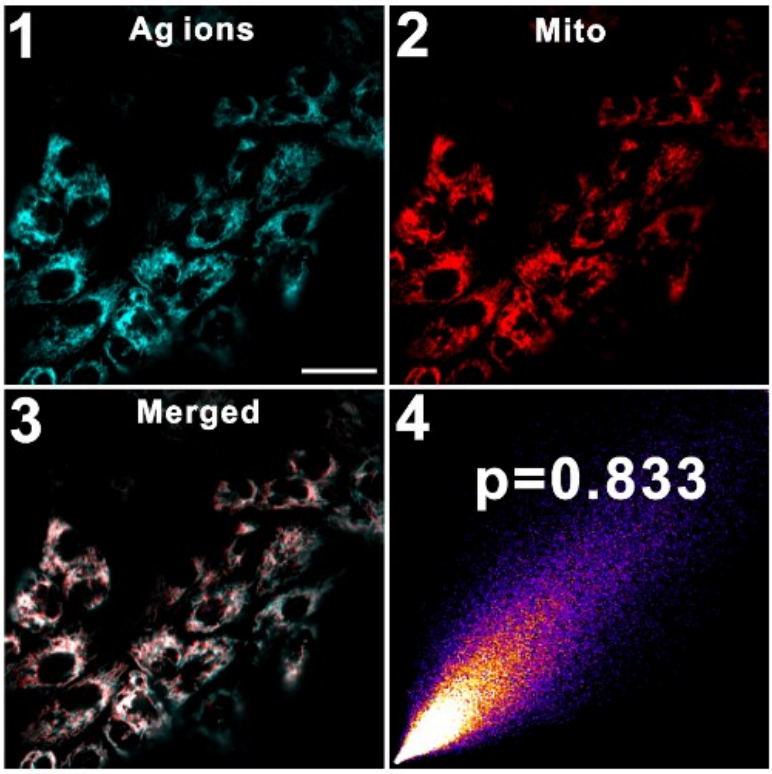

Figure S11. Confocal images of ZF4 cell lines exposed to Cit-AgNPs and mitochondria tracker.

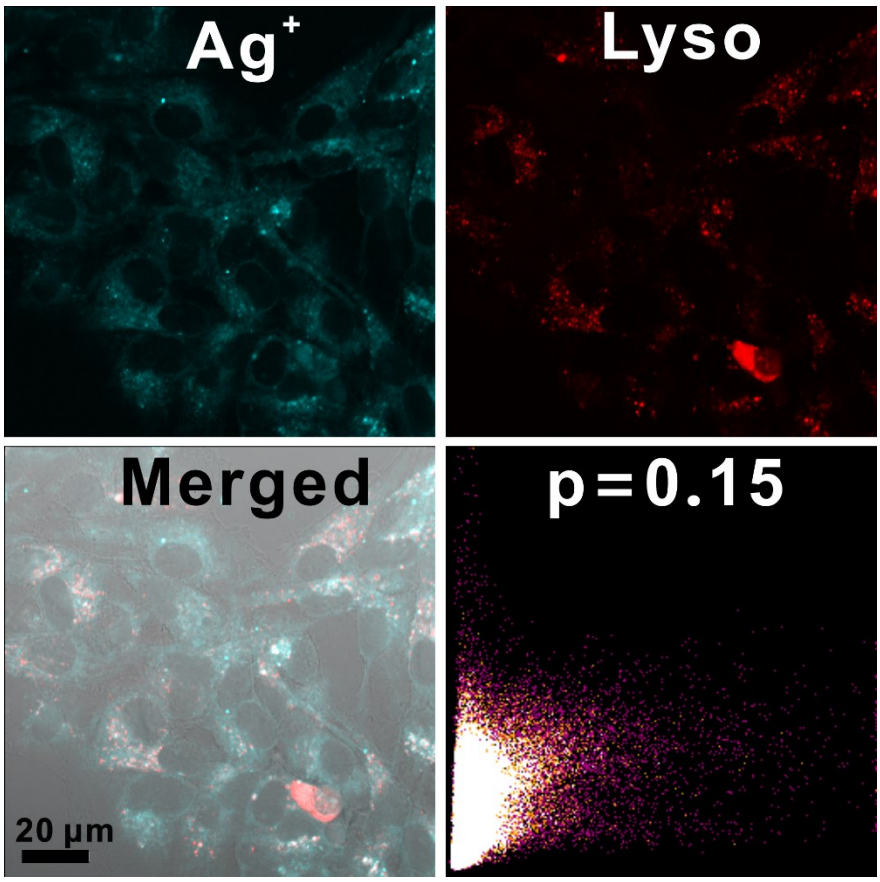

Figure S12. Confocal images of Ag^+ and lysosomes, and their corresponding colocalization analysis.

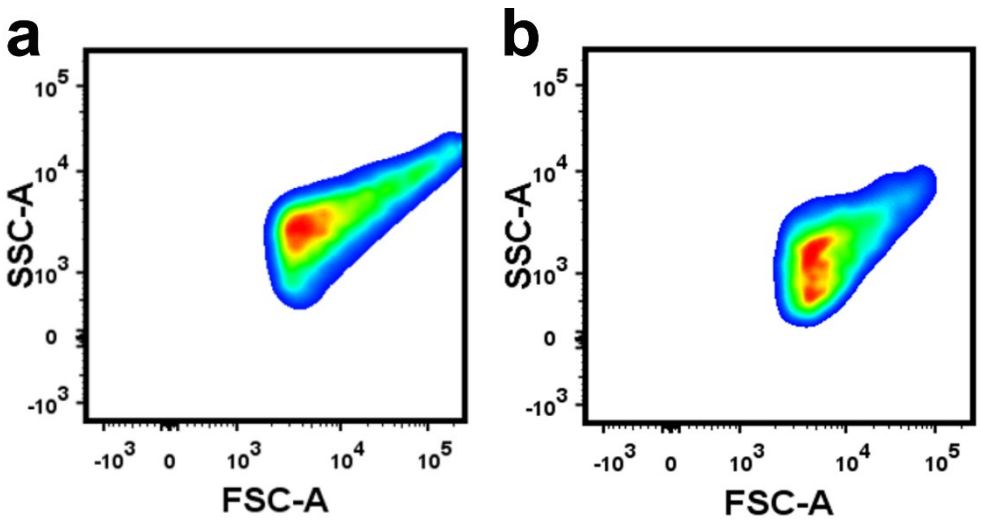

Figure S13. Representative scatter plot of ZF4 cell lines, FSC (forward scatter, OX- axis) provides information on the relative size of the analyzed events, while SSC (side scatter, OY-axis) estimates the granularity. (a) Flow cytometry analysis of ZF4 cell lines treated with 1 mg/L of Ag^+ for 24 h. (b) Flow cytometry analysis of ZF4 cell lines treated with 1 mg/L of AIE-AgNPs for 24 h.

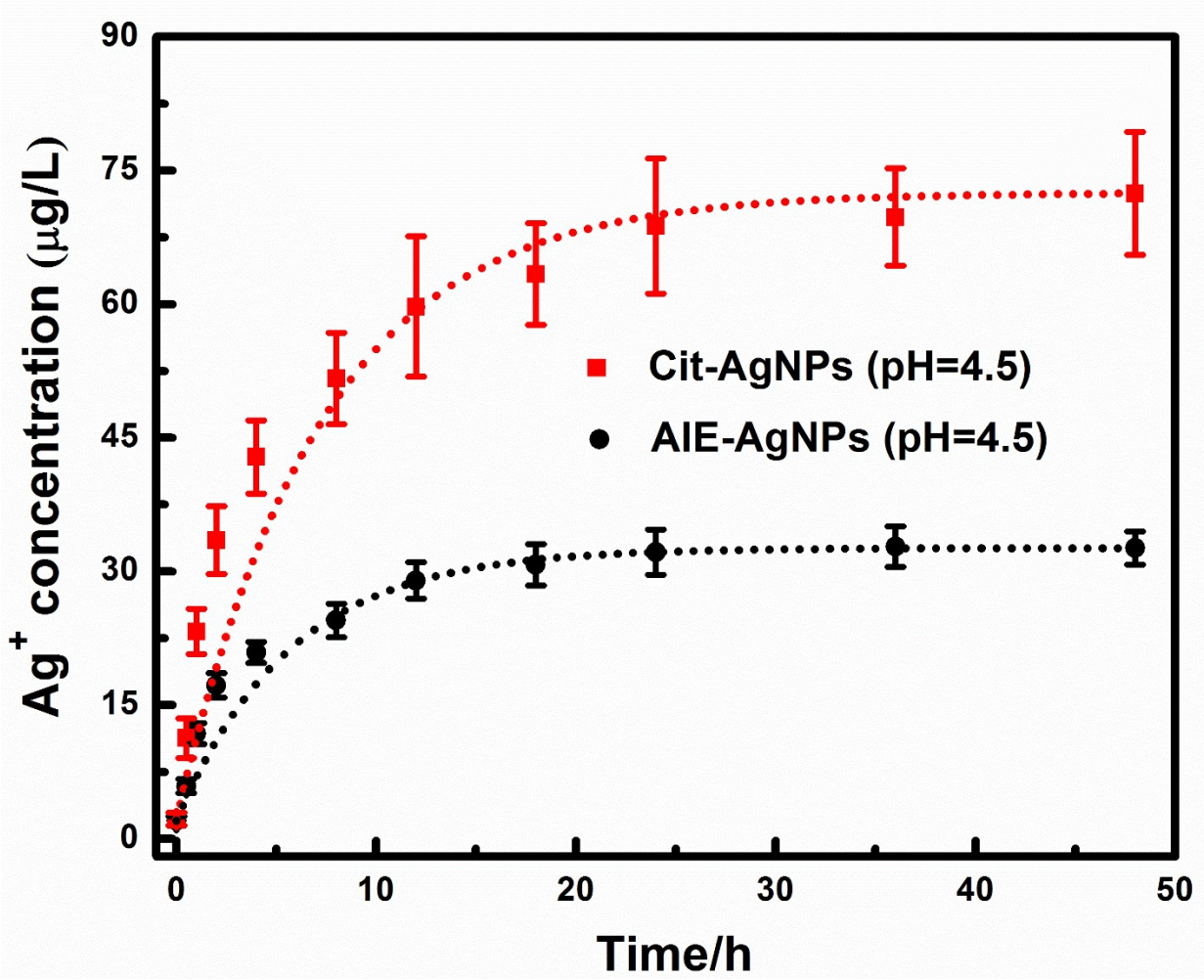

Figure S14. Dissolution kinetics of 500 μg/L of Cit-AgNPs-1 and AIE-AgNPs-1 in SM7 medium (pH=4.5).

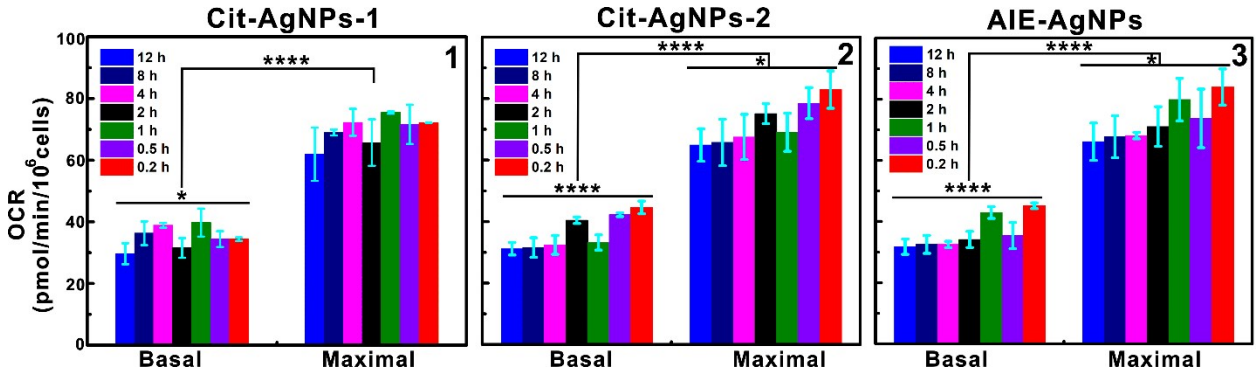

Figure S15. Oxygen consumption rate (OCR) measured by Seahorse MitoStress assay of cells exposed to Cit-AgNPs-1 (1), Cit-AgNPs-2 (2) and AIE-AgNPs (3) at different time points.

Reference

1. Braun, G. B.; Friman, T.; Pang, H. B.; Pallaoro, A.; Hurtado de Mendoza, T.; Willmore, A. M.; Kotamraju, V. R.; Mann, A. P.; She, Z. G.; Sugahara, K. N.; Reich, N. O.; Teesalu, T.; Ruoslahti, E., Etchable plasmonic nanoparticle probes to image and quantify cellular internalization. *Nat. Mater.* **2014,** *13* (9), 904-11.

2. Piao, M. J.; Kang, K. A.; Lee, I. K.; Kim, H. S.; Kim, S.; Choi, J. Y.; Choi, J.; Hyun, J. W., Silver nanoparticles induce oxidative cell damage in human liver cells through inhibition of reduced glutathione and induction of mitochondria-involved apoptosis. *Toxicol. Lett.* **2011,** *201* (1), 92-100.

3. Ghosh, M.; Manivannan, J.; Sinha, S.; Chakraborty, A.; Mallick, S. K.; Bandyopadhyay, M.; Mukherjee, A., In vitro and in vivo genotoxicity of silver nanoparticles. *Mutation Research/Genetic Toxicology and Environmental Mutagenesis* **2012,** *749* (1-2), 60-69.

4. Lv, X.; Wang, P.; Bai, R.; Cong, Y.; Suo, S.; Ren, X.; Chen, C., Inhibitory effect of silver nanomaterials on transmissible virus-induced host cell infections. *Biomaterials* **2014,** *35* (13), 4195-4203.